Preliminary characterisation of $LiAsF_6$ hybrid polymer electrolytes for electrochromic devices

L. C. Rodrigues[a], M. M. Silva[a1], M. J. Smith[a], A. Gonçalves[b], E. Fortunato[b]

[a]*Centro de Química, Universidade do Minho, Gualtar, 4710-057 Braga, Portugal*

[b]*CENIMAT/I3N, Departamento de Ciência dos Materiais, Faculdade de Ciências e Tecnologia, FCT, Universidade Nova de Lisboa e CEMOP-UNINOVA, 2829-516 Caparica, Portugal*

[1]nini@quimica.uminho.pt

Abstract

In this exploratory study the results of characterisation of a poly(oxyethylene) (PEO)/siloxane hybrid network electrolyte doped with lithium hexafluoroarsenate ($LiAsF_6$) are described. In accordance with convention, the lithium salt concentration is expressed in terms of the number of oxyethylene units in the organic component of the host network per Li^+ ion guest species.

Samples of solvent-free electrolytes were prepared with a range of guest salt concentration using the sol-gel process. Hybrid materials based on $LiAsF_6$, were obtained as mechanically robust, flexible, transparent and completely amorphous films and characterized by conductivity measurements, thermal analysis and electrochemical stability.

Preliminary characterisation of electrochromic devices (ECDs) incorporating optimised $LiAsF_6$-doped di-ureasil compositions have confirmed that these electrolytes perform satisfactorily as multifunctional component layers in this application.

1 ISE member

1. Introduction

According to Judeinstein and Sanchez's classification [1], hybrid materials in which the organic and inorganic components are linked by strong chemical bonds are designated as Class II hybrids. Several new classes of materials with novel physical and chemical properties have been synthesised by different routes using a combination of organic and inorganic segments [2]. These materials are of increasing interest because of potential applications in technologically-demanding areas including optical coatings, contact lenses and electrochromic displays [3-6]. Owing to its high versatility, the sol-gel method offers important advantages for the preparation of this class of materials [7]. There is a wide choice of metal alkoxide precursors that allow the preparation of matrices with different physical and chemical properties.

The development of electrochromic (EC) materials is an exciting and rapidly-expanding field of research [8]. Electrochromism may be defined as a persistent and reversible switch of colour (typically from a transparent or "bleached" state to a coloured or "written" state) in response to an electrochemical change.

A conventional electrochromic device (ECD) is composed of three elements arranged in a layered, "sandwich"-type configuration in which an EC electrode and a counter-electrode (CE) are physically separated, but ionically connected, by a liquid or solid (e.g., polymer) electrolyte. Colour changes occur by charging/discharging this electrochemical cell through the application of an electrical potential. A common feature of ECDs is that once they are coloured, the activating voltage can be switched off and the colour retained (memory effect), making them more energy efficient.

In recognition of their potential application in ECDs, we have prepared d-U(2000)-based hybrid electrolytes with a wide range of $LiAsF_6$ concentrations and characterised their ionic conductivity, electrochemical stability and thermal behaviour.

2. Experimental

2.1 Materials

Lithium hexafluoroarsenate ($LiAsF_6$, Aldrich, 99.998%) was used without further purification and stored prior to use in a high integrity, dry argon-filled glovebox.

The O,O'- diamine poly(oxyethylene-co-oxypropylene) (commercially available from Fluka as Jeffamine ED-2001®, average molecular weight 2001 $gmol^{-1}$) was dried under vacuum at 25ºC for several days prior to use. The bridging agent, 3-isocyanatepropyltriethoxysilane (ICPTES, Aldrich 95 %), was used as received. Ethanol (CH_3CH_2OH, Merck, 99.8%) and tetrahydrofuran (THF, Merck, 99.9%) were dried over molecular sieves. High purity distilled water was used in all experiments.

2.2.1 Preparation of the di-ureasil ormolytes

The synthetic procedure used to prepare the $LiAsF_6$-based diureasils was based on an optimised two-step method previously described in detail elsewhere [9]. The experimental procedure involves grafting a PEO-based diamine onto the ICPTES substrate to yield the di-urea-bridged hybrid precursor. This grafting process was monitored by IR spectroscopy. As the reaction proceeds the very strong, narrow absorption band located at ca. 2274 cm^{-1}, assigned to the vibration of the isocyanate group of the ICPTES molecule, becomes progressively less intense, while the bands due to the presence of urea cross-links absorb more strongly. This intermediate material was subsequently hydrolysed and condensed in the sol–gel stage to induce growth of the siloxane network.

Step 1. Synthesis of the di-ureasil precursor, d- UPTES(2000)

2.0 g of Jeffamine ED-2001 were dissolved in 10 ml of THF with stirring. A volume of 0.494 ml of ICPTES was added to this solution in a fume cupboard. The reaction flask was sealed and the solution stirred for about 12 h at a moderate reaction temperature of approximately 40ºC. A urea bridged organic/inorganic hybrid material, designated as di-ureapropyltriethoxysilane (d-UPTES(2000)), was obtained under these conditions.

Step 2. Synthesis of the di-ureasil xerogels, d-U(2000)$_n$LiAsF$_6$

A volume of 0.467ml of ethanol, an appropriate mass of $LiAsF_6$ and 0.054ml of water were added to the d-UPTES(2000) solution prepared in the previous step (molar proportion 1 d-UPTES(2000):4CH_3CH_2OH:1.5H_2O). The mixture was stirred in a sealed flask for approximately 30min, cast into a Teflon mould, covered with Parafilm and left in a fume cupboard for 24 h. The mould was transferred to an oven at 50ºC and the sample was aged for a period of 4 weeks. These films were subsequently transferred to a Buchi TO51 oven, where residual solvent was removed over a period of 3 days. During this period the temperature of the tube oven was raised from 30 to 90^{o}C and the oven was periodically evacuated and purged with dry argon. The ormolytes were identified using the notation d-U(2000)$_n$LiAsF$_6$, where d-U(2000) represents the host di-ureasil framework (d stands for di, U denotes the urea group and 2000 corresponds to the average molecular weight of the organic precursor) and n (salt composition) indicates the number of ether oxygen atoms per Li^+ cation.

2.2. Measurements

2.2.1. DSC and TGA measurements

Hybrid electrolyte sections were removed from cast films and subjected to DSC analysis under a flowing argon atmosphere between 25 and 300^{o}C at a heating rate of

$5^{o}C.min^{-1}$ using a Mettler DSC 821e. All samples were presented for analysis in 40 µL aluminium cans with perforated lids to permit the release and removal of the decomposition products. Samples for thermogravimetric studies were prepared in a similar manner, transferred to open platinum crucibles and analysed using a Rheometric Scientific TG 1000 thermobalance operating under a flowing argon atmosphere. A heating rate of $10^{o}Cmin^{-1}$ was used to analyse all the hybrid samples.

2.2.2. Impedance spectroscopy

Total ionic conductivities of hybrid samples were determined using a constant volume support equipped with gold blocking electrodes and located within a Buchi TO 50 oven. The sample temperature was evaluated by means of a type K thermocouple placed close to the electrolyte film and impedance measurements were carried out at frequencies between 65kHz and 500mHz using an Autolab PGSTAT-12 (Eco Chemie), over a temperature range from 20 to $90^{o}C$. Measurements of conductivity were effected during heating cycles. The reproducibility of recorded conductivities was confirmed by comparing the results obtained for a sample subjected to two heating-cooling-heating cycles. The excellent reproducibility of the results obtained using this procedure demonstrated the correct operation of the support and the mechanical stability of the samples.

2.2.3. Electrochemical stability

Evaluation of the electrochemical stability window of hybrid compositions was carried out within a dry argon-filled glovebox using a two-electrode cell configuration. The preparation of a 25µm diameter gold microelectrode surface by the conventional polishing routine was completed outside the glove box. The microelectrode was then

washed with THF, dried with a hot-air blower and transferred to the interior of the glove box. Cell assembly was initiated by locating a freshly-cleaned lithium disk counter electrode (10 mm diameter, 1mm thick, Aldrich, 99.9% purity) on a stainless steel current collector. A thin-film sample of d-U(2000)$_n$LiAsF$_6$ was centered over the counter electrode and the cell assembly completed by locating and supporting the microelectrode in the centre of the electrolyte disk. The assembly was held together firmly with a clamp and electrical contacts were made to the Autolab PGSTAT-12 potentiostat used to record voltammograms at a scan rate of 100 mVs^{-1}. All measurements were conducted at room temperature within a Faraday cage located inside the dry argon-filled glovebox.

2.2.4. Assembly and characterization of the ECDs

Indium zinc oxide (IZO) films were deposited on glass substrates by r.f. (13.56 MHz) magnetron sputtering using a ceramic oxide target In_2O_3:ZnO (92:8 wt%; 5 cm diameter, Super Conductor Materials, Suffern, NY, U.S.A., purity of 99.99%). Sputtering was carried out at room temperature, with an argon flow of 20 cm^3/min and an oxygen flow of 0.4 cm^3/min. During sputtering the total deposition pressure (argon and oxygen) was held constant at 0.15 Pa. The distance between the substrate and the target was 10 cm and the r.f. power was maintained at 100 W. WO_3 (Super Conductor Materials, purity of 99.99%) films with thickness of about 300 nm were deposited on the transparent conductive oxide IZO-coated glass substrates by r.f. magnetron sputtering (Pfeiffer Classic 500). Sputtering was carried out at room temperature, under an argon and oxygen atmosphere with a constant deposition pressure of 2.6 Pa. The distance between the substrate and the target was 10 cm and the r.f. power was

maintained at 200 W. The thicknesses of the WO_3 and IZO layers on the WO_3/IZO-coated glass plate were 400 nm and 170 nm, respectively.

All-solid-state ECDs were constructed using the four-layer sandwich configuration glass/IZO/WO_3/d-U(2000)$_n$LiAsF_6/IZO/glass. Device assembly with the EC layer was carried out by direct application of a small volume of the ormolyte sol to the surface of the WO_3/IZO-coated glass plate. After a period of about 24h the IZO-coated glass plate was placed on top of the resulting ormolyte gel and the two plates were pressed together so that the two coated faces bonded together inside the assembled system. In this manner a thin electrolyte layer with a surface area of approximately 2 cm^2 was formed. A strip of contact area was left uncoated on each side of the glass slide in order to make electrical contacts to the external circuit. The entire assembly procedure described in this section was carried out under atmospheric conditions.

3. Results and discussion

3.1. Thermal behaviour of electrolytes

Analysis of the thermograms of the d-U(2000)$_n$LiAsF_6 electrolytes represented in Fig. 1 leads us to conclude that these materials are semi-crystalline over the range of compositions studied. The endothermic peak located close to 50ºC, more evident in the thermograms of the less concentrated samples, is attributed to the fusion of PEO spherulites [10]. The onset temperature of thermal decomposition was estimated by thermogravimetric analysis using extrapolation of the baseline and tangent of the curve of thermal events to identify the initiation of sample weight loss (Fig 2). The results of DSC and TGA analysis are consistent with a minimum thermal stability of about 255ºC

for the n = 2.5 electrolyte composition (Fig. 1 and 2), a value considered acceptable for applications in EC displays under normal operating conditions. The results presented in Fig. 2 show a clear decrease in thermal stability with increasing salt concentration, confirming that the salt has a destabilizing influence on the hybrid matrix host (this behaviour is similar to that reported for d-U(2000)$_n$LiClO$_4$ ormolytes [11]). The absence of weight loss in the TGA curves confirm that there are no thermal events associated with residual solvent evaporation (water, ethanol or THF).

Ionic mobility in an electrolyte is largely determined by the relaxation modes of the polymer host. Lower values of T_g indicate that the local chain segment motion of the host polymer in the electrolyte system is less constrained by intermolecular interactions. The T_gs of various compositions of d-U(2000)$_n$LiAsF$_6$ ormolytes are identified in Fig. 3, and it may be clearly seen that values of Tg are shifted to higher temperatures when the salt content is increased. For compositions with n≥8 the values of Tg remain almost constant and this observation confirms that the PEO chains of the d-U(2000)$_n$LiAsF$_6$ matrix are not significantly constrained by coordination with the guest lithium ions in this range of composition and that the cation/polymer interactions in these samples do not significantly influence the T_g values. This effect was also observed in previous studies of other hybrid organic-inorganic systems [11]**.**

In salt-rich compositions the increase in Tg is greater than 20ºC and the poor mechanical properties of these compositions preclude their use in practical devices. At salt content of n = 2.5 films were not flexible and fragmented when subjected to mechanical stress.

The hybrid matrices described in this study are complex three-dimensional structures that are significantly influenced by the chemical composition of the reaction mixture during the sol-gel process. Although the synthetic procedure was closely controlled and

reproducible sample characteristics were obtained, the impact of factors including residual water, or HF residues produced during synthesis, is not yet clear. These factors may play an important role in determining the mechanical behaviour, and therefore electrochemical properties, of electrolyte formulations. Future characterisation with Raman Spectroscopy may help to provide additional information to clarify this aspect of these materials.

3.2. Ionic conductivity of electrolytes

The ionic conductivities of various hybrid electrolyte compositions over the temperature range from 25 to 90 ºC, and as a function of salt content (n from 2.5 to 200), are illustrated in Fig. 4a) and b). This behaviour contrasts with that of semi-crystalline materials based on the PEO host matrix that often show two distinct linear segments with a change of gradient close to the melting temperature of PEO spherulites. The sol-gel electrolytes are significantly more amorphous than the PEO-based materials, with a lower activation energy for ion transport. With the d-U(2000)$_n$LiAsF$_6$ system, as the crystalline component of the electrolyte melts at close to room temperature, the conductivity curves exhibit the non-linear behaviour typical of amorphous morphology.

From the results presented in Fig. 4 it is evident that the most conducting sample of the series is d-U(2000)$_{30}$LiAsF$_6$. At about 25ºC, this electrolyte composition presents a conductivity of 7.69x10^{-6} Scm^{-1}, and at 90ºC 2.41x10^{-4} Scm^{-1}, values similar to that reported by Nunes *et al* [12] for d-U(2000)$_{20}$ LiCF$_3$SO$_3$ were observed. These electrolytes supported higher total ionic conductivity than systems based on PEO [13]. This result was expected, as the PEO-based electrolytes are generally poor conductors at ambient temperature due to the presence of crystalline material. The conductivity

results, included in Fig. 4, confirm that this electrolyte system behaves in a similar manner to that reported for other ormolytes systems [14-16]. As the mechanism of ionic transport is depends on the flexibility of the polymer chain, components that increase free volume may be expected to have a beneficial influence on conductivity. A further increase in salt content, beyond the salt composition associated with the electrolyte with the lowest T_g, results in an increase in the energy required for chain rotation and a decrease in the segment mobility. Restrictions in the motion of the polymer chain segments, responsible for ion transport, explain the sudden decrease in conductivity at high salt content, a fairly common observation in solvent-free polymer electrolyte systems.

3.3. Electrochemical stability

The electrochemical stability of the d-U(2000)$_8$LiAsF$_6$ and d-U(2000)$_{20}$LiAsF$_6$ electrolyte was determined by microelectrode cyclic voltammetry over the potential range -2.0 to 6.0 V (Figure 5). The potential limit for the electrolyte composition was determined as the potential at which a rapid rise in current was observed and where the current continued to increase as the potential was swept in the same direction. On the cathodic sweep a low current peak at approximately 4.0V vs. Li/Li$^+$ was observed and attributed to the reduction of decomposition products that were formed at the anodic limit. Lithium deposition begins in the cathodic region at about –1.0 V vs. Li/Li$^+$. The overall stability of the electrolyte is good with no electrochemical oxidation occurring at potentials less than 5.0 V. This result confirms that the electrolyte system has adequate electrochemical stability for application in electrochromic displays or practical primary and secondary cells.

3.4. Electrochromic device operation

The structure of the prototype solid-state electrochromic device is represented in Figure 6. The colouring and bleaching voltages were 3 V and -1.5 V and were applied for periods of about 20 and 10 seconds respectively. The active layer of the assembled device changed from almost transparent to a blue colour associated with WO_3 reduction and simultaneous Li^+ insertion as a result of the application of a positive voltage. Inversion of the applied voltage resulted in WO_3 oxidation and the device returned to its initial state. The images included in Figure 7 illustrate the optical transmittance in the wavelength range 300–900nm for the devices based on d-U(2000)$_n$LiAsF$_6$ di-ureasils. It is evident that the electrochromic device strongly absorbs ultraviolet radiation below 350 nm in both its bleached and coloured states. Table 1 summarises the average transmittance and the optical density exhibited by the electrochromic display element. The average transmittance in the visible region of the spectrum was around 60% for all the bleached samples analysed. After colouration the ECD structure assembled with the d-U(2000)$_{20}$ LiAsF$_6$ ormolyte showed a colour contrast of about 18% and an OD of 0.21 (Table 1), thus providing a good performance in the colouring/bleaching process (Figure 6 and 7). The displays assembled with an electrolyte film composition of n = 8 recorded an optical density above 0.45, providing an excellent performance in colouring/bleaching process (Figures 6 and 7). For a prototype ECD based on the d-U(2000)$_{20}$KCF$_3$SO$_3$ [16] di-ureasil the average transmittance in the visible region is situated at 85-95 % for the bleached state, while for the coloured state the di-ureasil presents a transmittance around 90%. The d-U(2000)$_n$LiTFSI [17] showed an average transmittance in the visible region of the spectrum above 70% for all the bleached samples analysed.

The average transmittance in the visible region of the spectrum was above 69% for devices based on d-U(900)$_5$LiTFSI and was above 74% for devices based on d-U(600)$_{25}$LiBF$_4$ di-ureasils [18]. After colouration the device based on d-U(900)$_5$LiTFSI presented a good colour contrast (above 24%) and an optical density above 0.49, and the device based on d-U(600)$_{25}$LiBF$_4$ presented an average transmittance of 48% and an optical density above 0.17, providing a good performance in the colouring/bleaching process. These results are very satisfactory, especially when compared to those obtained with d-U(900)$_n$LiClO$_4$ electrolytes [19]. The reasons for the variation of optical density with electrolyte composition are not yet clear and require further study. These findings are consistent with mechanical interfacial effects or the supply of ions due to higher ionic conductivity, both aspects of electrolyte performance that vary significantly with composition.

One of the advantages of electrochromic over liquid crystal displays is the storage property of the electrochromic device in an open circuit condition. All the devices characterised demonstrated good stability and good storage properties. This study confirms that the optical behaviour of the prototype electrochromic devices assembled with this hybrid organic-inorganic electrolyte is superior to that of other hybrid matrices [17].

4. Conclusions

A family of organic-inorganic hybrid materials, designated as d-U(2000)$_n$LiAsF$_6$, with a wide range of salt concentration, was prepared by the sol-gel method. The assembly of all-solid-state devices using these polymeric electrolytes represents an advance in the sense that they improve specific operational characteristics

and may also provide useful additional adhesive or sealing functions. The common failure modes caused by electrolyte loss or reaction with active electrode material are examples of problems associated with the use of liquid electrolytes in electrochromic devices that are eliminated by the application of polymer electrolytes in these devices.

The encouraging results observed in this exploratory study confirm the advantages that derive from the use of the d-U(2000)$_n$LiAsF$_6$ di-ureasil matrices in ECDs. Clearly further optimisation of the synthesis of the hybrid matrix and device assembly procedures is required. One of the greatest advantages of the sol-gel process is the possibility of tailoring the final product through a precise control of the reaction mixture during synthesis. The influence of water, HF and salt content on the structure of the final matrix has not yet been clarified, however spectroscopic studies are currently being undertaken with this objective. A better understanding of the synthetic process will certainly lead to improvements in electrolyte performance and therefore a reduction in device response time and greater display colour uniformity may be expected.

Acknowledgements

The authors are pleased to acknowledge the financial support provided by the University of Minho and the *Fundação para a Ciência e Tecnologia* (contracts POCTI/SFA/3/686 and SFRH/BD/38616/2007) for laboratory equipment and research staff.

List of figure captions

Figure 1. DSC thermograms of selected d-U(2000)$_n$LiAsF$_6$ hybrids.

Figure 2. TGA curves of d-U(2000)$_n$LiAsF$_6$ hybrids.

Figure 3. Tg and the percent of crystalline of selected d-U(2000)$_n$LiAsF$_6$ hybrids.

Figure 4. Variation of ionic conductivity with 1/*T* for selected hybrid compositions of d-U(2000)$_n$LiAsF$_6$.

Figure 5. Voltammogram of d-U(2000)$_8$LiAsF$_6$ and d-U(2000)$_{20}$LiAsF$_6$ electrolytes at a 25µm diameter gold microelectrode versus Li/Li$^+$. Initial sweep direction is anodic and sweep rate is 100mVs^{-1}.

Figure 6. Electrochromic device in bleached and coloured states at selected compositions: **a)** d-U(2000)$_8$LiAsF$_6$, **b)** d-U(2000)$_{20}$LiAsF$_6$.

Figure 7. Optical transmittance as a function of wavelength for the electrochromic device in bleached and colored state using (a) d-U(2000)$_8$LiAsF$_6$; (b) d-U(2000)$_{20}$LiAsF$_6$.

Tables

Table 1- Average transmittance and optical density exhibited by electrochromic devices using d-U(2000)$_8$LiAsF$_6$ and d-U(2000)$_{20}$LiAsF$_6$.

References

[1] P. Judeinstein, C. Sanchez, J. Mater. Chem. 6 (1996) 511.

[2] D. A. Loy, K. J. Shea, Chem. Rev. 95 (1995) 1431.

[3] C. M. Lampert, Solar Energy Mater. Solar Cells 52 (1998) 207.

[4] E. Syrrakou, S. Papaefthimiou, P. Yianoulis, Solar Energy Mater. Solar Cells 85 (2005) 205.

[5] T. Lukaszewicz, A. Ravinski, I. Makoed, Nonlinear Analysis: Modelling and Control 9 (2004) 363.

[6] C. Sanchez, B. Julián, P. Belleville, M. Popall, J. Mater. Chem. 15 (2005) 3559.

[7] C.J. Brinker, G. Scherer, Sol-Gel Science: The Physics and Chemistry of Sol-Gel Processing, Academic Press, San Diego, CA, 1990.

[8] C. M. Lampert, A. Agrawal, C. Baertien, J. Nagai, Sol. Energy Mater. Sol. Cells 56 (1999) 449.

[9] S. M. G. Correia, V. de Zea Bermudez, M. M. Silva, S. Barros, R. A. Sá Ferreira, L. D. Carlos, A. P. Passos de Almeida, M. J. Smith, Electrochim. Acta, 47/15 (2002) 2421.

[10] L.D. Carlos, V. de Zea Bermudez, R. A. Sá Ferreira, L. Marques, M. Assunção, Chem. Mater. 11/3 (1999) 581.

[11] M. M. Silva, S. C. Nunes, P. C. Barbosa, A. Evans, V. de Zea Bermudez, M. J. Smith, D. Ostrovskii, Electrochim. Acta 52 (2006) 1542.

[12] S. C. Nunes, V. de Zea Bermudez, D. OstrovskiI, M. M. Silva, S. Barros, M. J. Smith, R. A. Sá Ferreira, L. D. Carlos, J. Rocha, E. Morales, J. Electrochem. Soc. 152 (2005) A429.

[13] M. Armand, J. M. Chabagno, M. Duclot, in Extended Abstracts Second International Conference on Solid Electrolytes, St Andrews, Scotland, 1978.

[14] S. C. Nunes, V. de Zea Bermudez, M. M. Silva, M. J. Smith, L. D. Carlos, R. A. Sá Ferreira, J. Rocha, J. Solid State Electrochem. 10 (4) (2006) 203.

[15] S. C. Nunes, V. de Zea Bermudez, D. Ostrovskii, P. B. Tavares, P. C. Barbosa, M. M. Silva, M. J. Smith, Electrochim. Acta 53 (2007) 1466.

[16] S. C. Nunes, V. de Zea Bermudez, M. M. Silva, M. J. Smith, D. Ostrovskii, R. A. Sá Ferreira, L. D. Carlos, J. Rocha J., A. Gonçalves, E. Fortunato, J. Mater. Chem. 17 (2007) 4239.

[17] P. C. Barbosa, M. M. Silva, M. J. Smith, A. Gonçalves, E. Fortunato, S. C. Nunes, V. de Zea Bermudez, Electrochim. Acta 54 (2009) 1002.

[18] L. C. Rodrigues, P. C. Barbosa, M. M. Silva, M. J. Smith, A. Gonçalves, E. Fortunato, Opt. Mater. 31 (2009) 1467.

[19] P. C. Barbosa, M. M. Silva, M. J. Smith, A. Gonçalves, E. Fortunato, Electrochim. Acta 52 (2007) 2938.

Figure 1

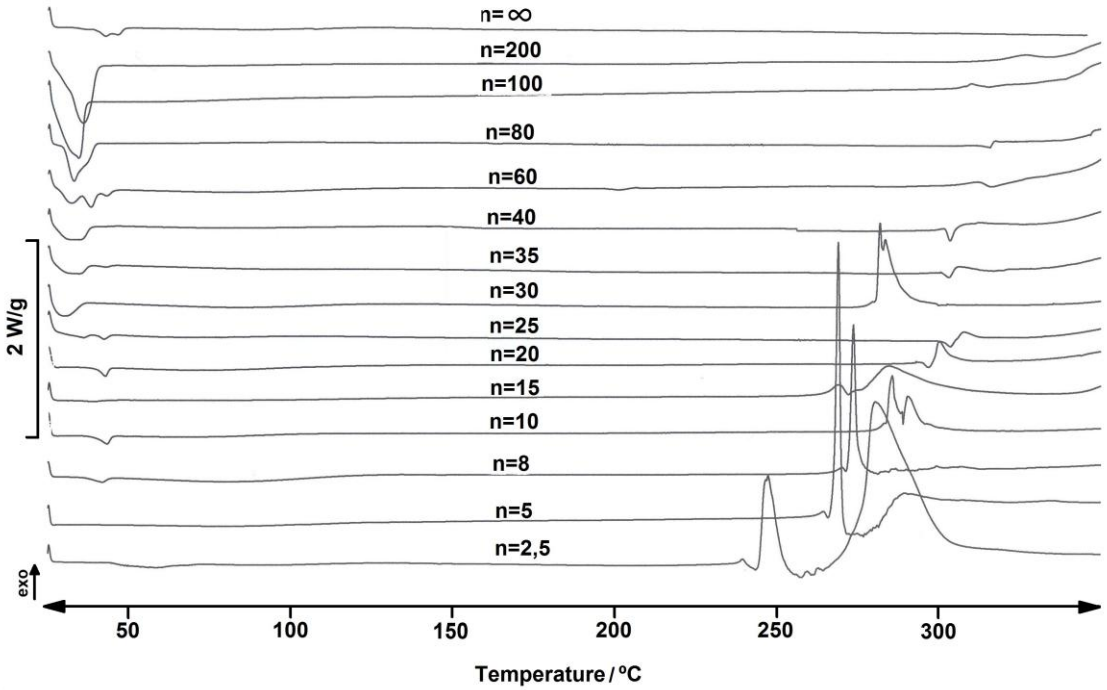
n=∞
n=200
n=100
n=80
n=60
n=40
n=35
n=30
n=25
n=20
n=15
n=10
n=8
n=5
n=2,5
2 W/g
exo
50
100
150
200
250
300
Temperature / °C

Figure 2

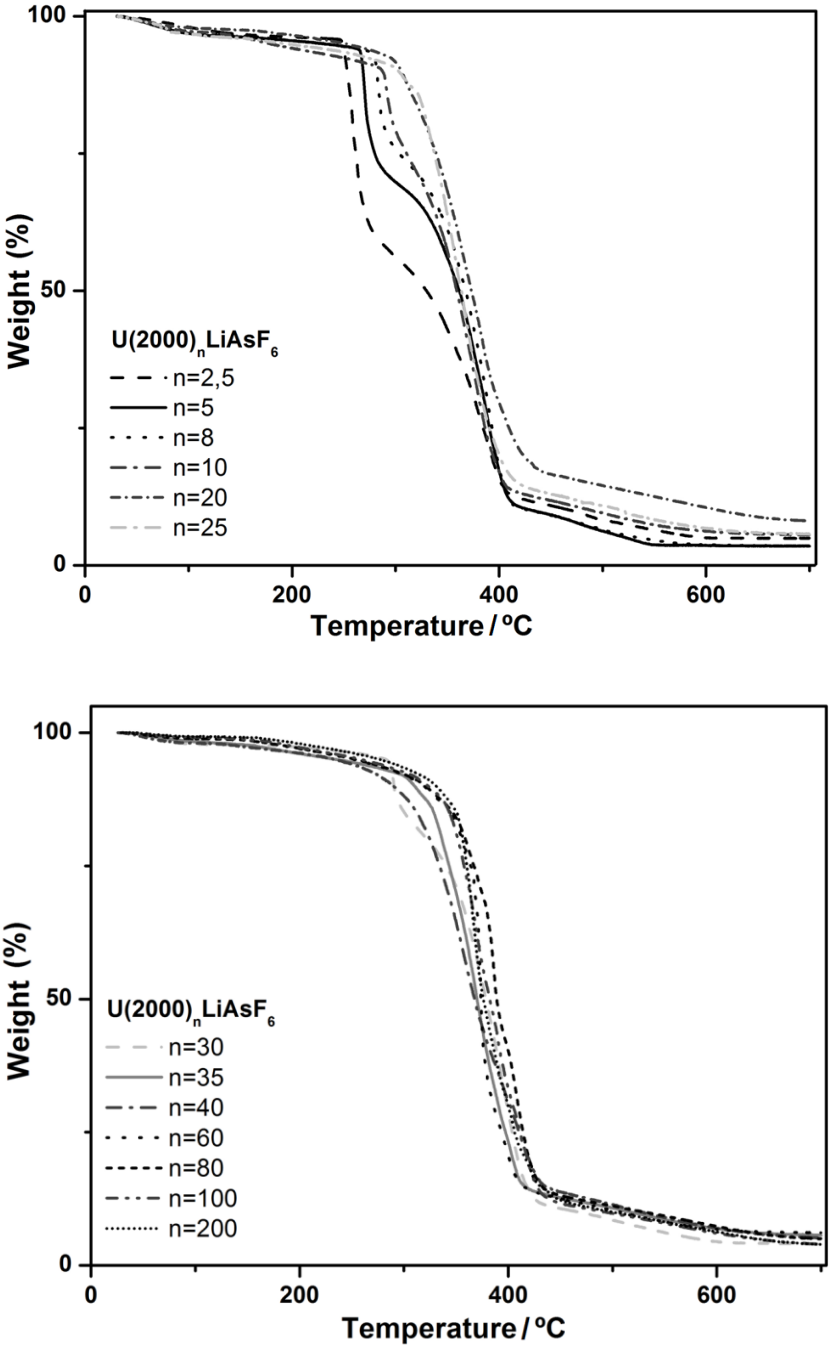
100
50
0
Weight (%)
0
200
400
600
Temperature / °C
U(2000)nLiAsF6
n=2,5
n=5
n=8
n=10
n=20
n=25
100
50
0
Weight (%)
0
200
400
600
Temperature / °C
U(2000)nLiAsF6
n=30
n=35
n=40
n=60
n=80
n=100
n=200

Figure 3

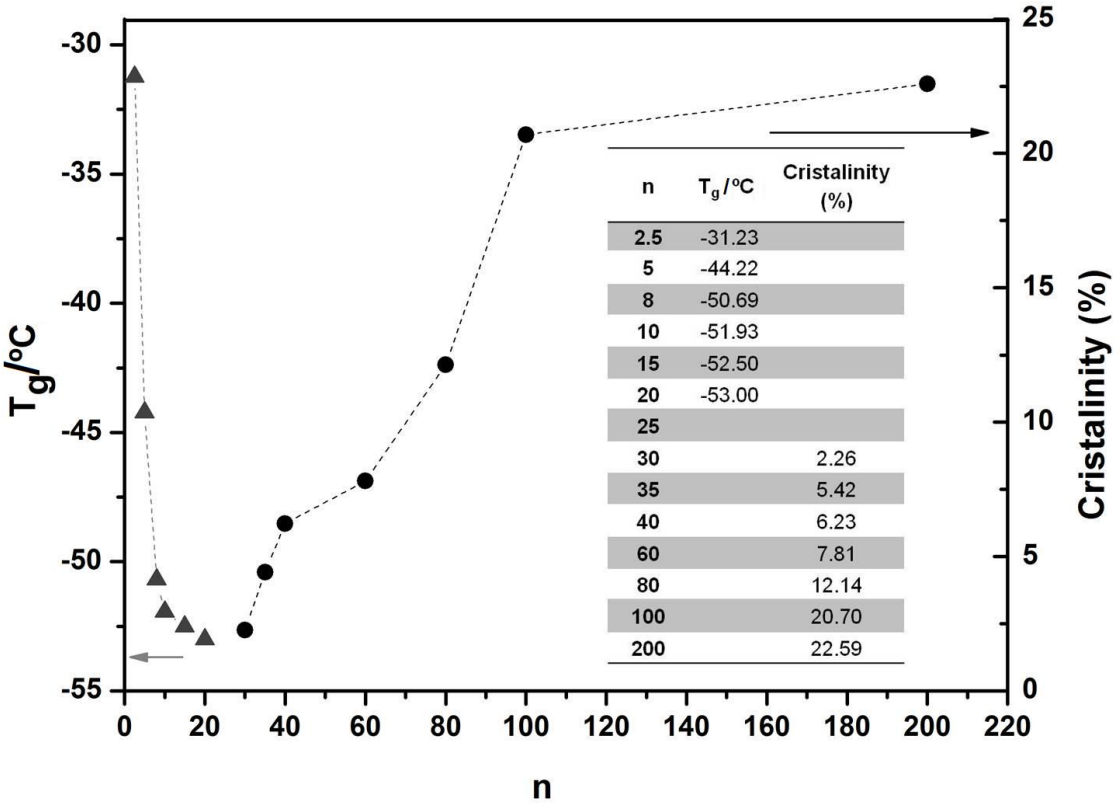

n	T_g/°C	Cristalinity (%)
2.5	-31.23	
5	-44.22	
8	-50.69	
10	-51.93	
15	-52.50	
20	-53.00	
25		
30		2.26
35		5.42
40		6.23
60		7.81
80		12.14
100		20.70
200		22.59

Figure 4

a)

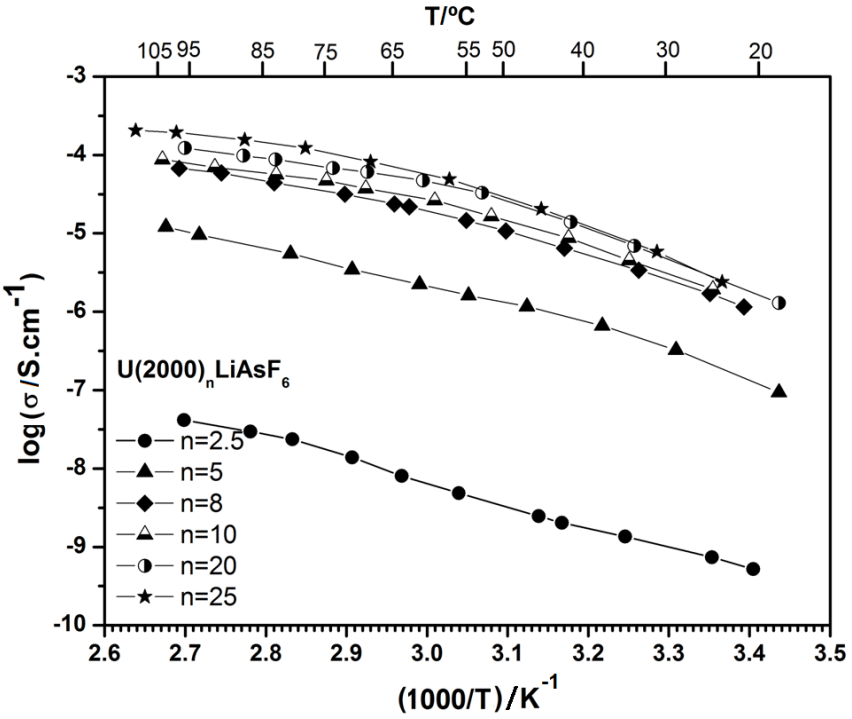
T/ºC
105 95 85 75 65 55 50 40 30 20
-3 -4 -5 -6 -7 -8 -9 -10
log(σ/S.cm-1)
U(2000)nLiAsF6
n=2.5
n=5
n=8
n=10
n=20
n=25
2.6 2.7 2.8 2.9 3.0 3.1 3.2 3.3 3.4 3.5
(1000/T)/K-1

b)

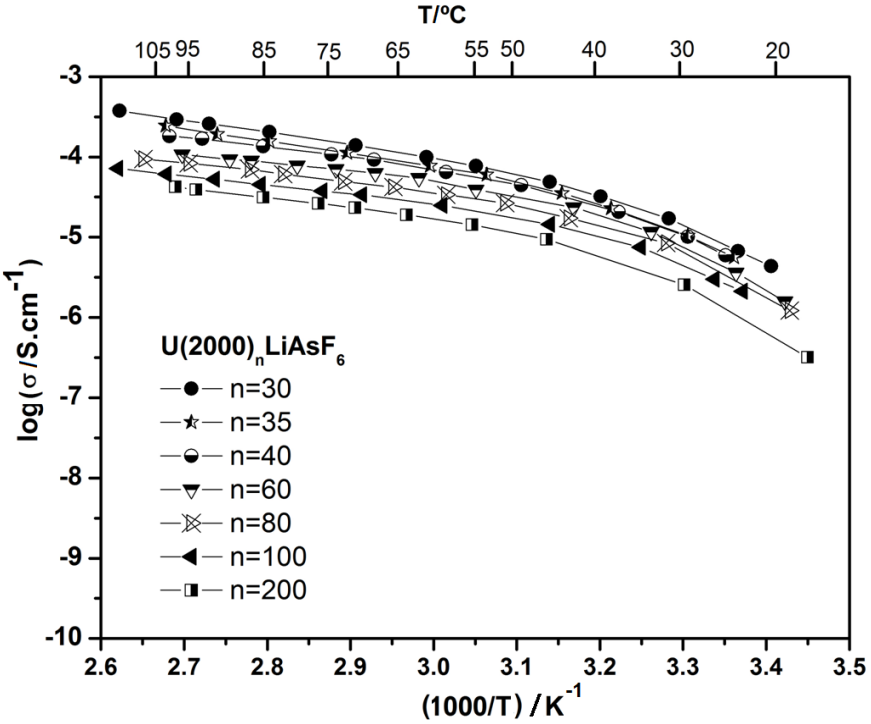
T/ºC
105 95 85 75 65 55 50 40 30 20
-3 -4 -5 -6 -7 -8 -9 -10
log(σ/S.cm-1)
U(2000)nLiAsF6
n=30
n=35
n=40
n=60
n=80
n=100
n=200
2.6 2.7 2.8 2.9 3.0 3.1 3.2 3.3 3.4 3.5
(1000/T)/K-1

Figure 5

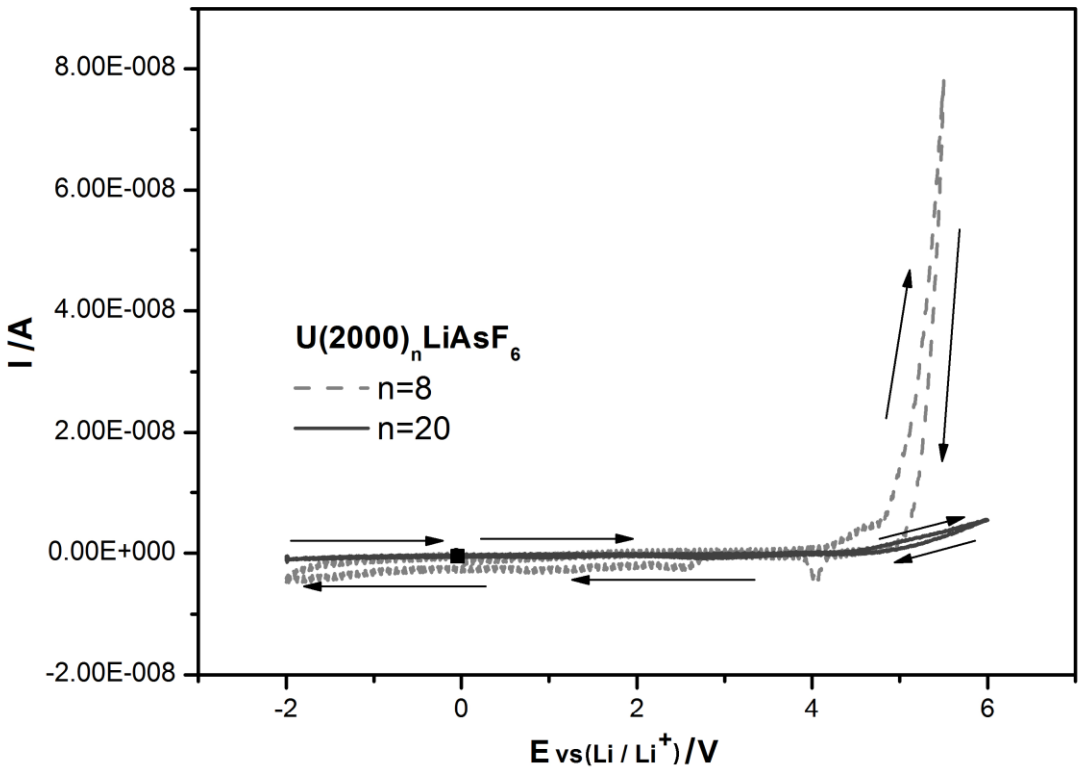
8.00E-008
6.00E-008
4.00E-008
2.00E-008
0.00E+000
-2.00E-008
I /A
U(2000)nLiAsF6
n=8
n=20
-2
0
2
4
6
E vs(Li / Li+) /V

Figure 6

a)


Universidade do Minho
Escola de Ciências
Universidade do Minho
Escola de Ciências
Departamento de Química

b)

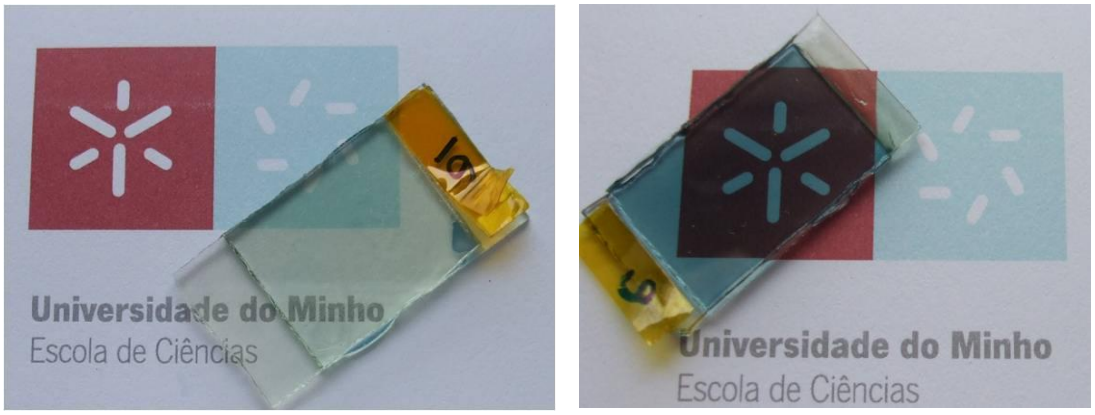
Universidade do Minho
Escola de Ciências
Universidade do Minho
Escola de Ciências

Figure 7

a)

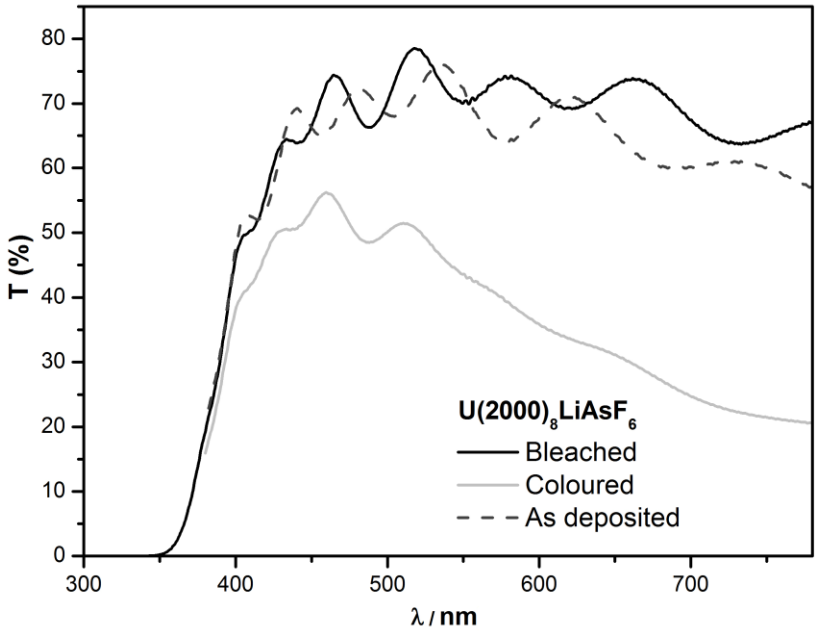
T (%)
λ / nm
U(2000)8LiAsF6
Bleached
Coloured
As deposited

b)

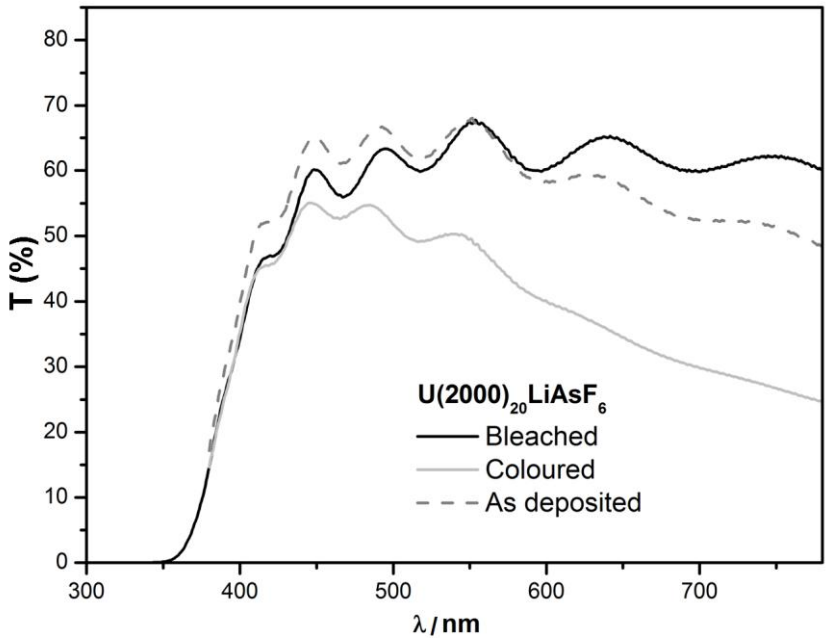
T (%)
λ / nm
U(2000)20LiAsF6
Bleached
Coloured
As deposited

Table 1

Sample	T Coloured state (%)	T Bleached state (%)	T As deposited (%)	Optical density
$U(2000)_8LiAsF_6$	36,82%	66,74%	63,27%	0,45
$U(2000)_{20}LiAsF_6$	39,78%	58,39%	56.45%	0,21